Contribution of positively charged flanking residues to the insertion of transmembrane helices into the endoplasmic reticulum

Mirjam Lerch-Bader, Carolina Lundin, Hyun Kim, IngMarie Nilsson, and Gunnar von Heijne*

Center for Biomembrane Research, Department of Biochemistry and Biophysics, Stockholm University, SE-106 91 Stockholm, Sweden

Edited by Richard Henderson, Medical Research Council, Cambridge, United Kingdom, and approved January 17, 2008 (received for review December 8, 2007)

Positively charged residues located near the cytoplasmic end of hydrophobic segments in membrane proteins promote membrane insertion and formation of transmembrane α-helices. A quantitative understanding of this effect has been lacking, however. Here, using an *in vitro* transcription–translation system to study the insertion of model hydrophobic segments into dog pancreatic rough microsomes, we show that a single Lys or Arg residue typically contributes approximately −0.5 kcal/mol to the apparent free energy of membrane insertion (ΔG_{app}) when placed near the cytoplasmic end of a hydrophobic segment and that stretches of 3–6 Lys residues can contribute significantly to ΔG_{app} from a distance of up to ≈13 residues away.

membrane protein | positive inside rule | hydrophobicity scale | translocon

The biosynthesis of α-helical membrane proteins requires their insertion, folding, and oligomerization in the target membrane. In eukaryotic cells, most membrane proteins insert cotranslationally into the endoplasmic reticulum (ER) membrane in a process mediated by the heterotrimeric Sec61 translocon (1, 2).

In a series of recent studies (3–6), we have determined the sequence characteristics responsible for the insertion of a transmembrane helix into the ER membrane by measuring the membrane-insertion efficiency of designed hydrophobic segments (H-segments) engineered into a model protein. The position-dependent apparent free energy of insertion derived from these studies for the different amino acids provides the basis for a truly "biological" hydrophobicity scale (6). The biological scale correlates well with biophysical and statistical hydrophobicity scales, such as the Wimley–White water–octanol partitioning scale (7) and Sansom's structure-based statistical scale (8). This correlation suggests that the insertion of transmembrane helices is largely determined by the thermodynamics of protein–lipid interactions (3), which is not unreasonable given the structure of the archeal Sec61 translocon in which a dynamic "lateral gate" may provide a polypeptide in transit ready access to the lipid bilayer (9, 10).

The biosynthesis of membrane proteins, however, not only requires the proper insertion of the transmembrane segments but also their correct orientation in the membrane, and the translocon is thought to play a pivotal role in this process as well (reviewed in ref. 11). Positively charged residues in membrane proteins are found predominantly on the cytoplasmic side of the membrane [the "positive inside" rule (12, 13)], flanking either signal sequences (14) or transmembrane segments (12). Consistent with this rule, positively charged residues favor insertion when placed at the cytoplasmic end of a transmembrane segment (6).

To characterize more fully the effects on membrane insertion of charged flanking residues, we have now measured the apparent free energy of membrane insertion of a set of H-segments with different combinations of charged flanking residues engineered into a model membrane protein. We have tested the effects of Lys and Arg residues by using simple Ala/Leu based H-segments and melittin-derived H-segments. Melittin, the main component of bee venom, is a cationic peptide composed of a predominantly hydrophobic stretch between residues 1 and 20 and a positively charged C-terminal region (residues 21–26) (15). A rich body of information has been collected in the last decades about its insertion into both model and natural membranes (for reviews, see refs. 16 and 17). Our results add an important element to ongoing efforts to provide a quantitative description of the relation between protein sequence and membrane insertion efficiency in helix bundle integral membrane proteins.

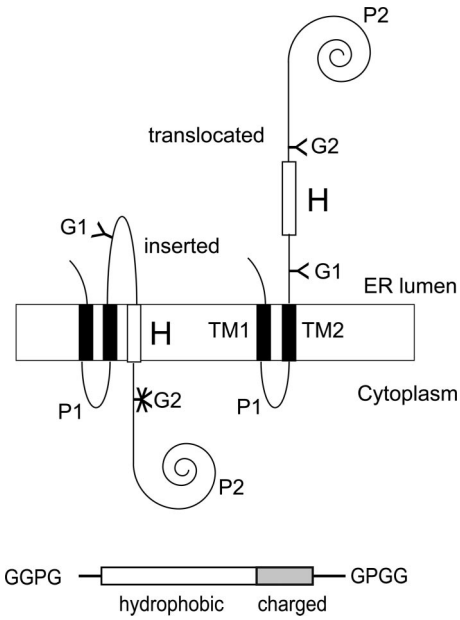

Fig. 1. Model protein. (*Upper*) (*Left*) If the H-segment forms a transmembrane helix, only the G1 acceptor site for N-linked glycosylation is modified by the luminal oligosaccharyl transferase. (*Right*) If the H-segment does not form a transmembrane helix, both the G1 and G2 acceptor sites are modified (3). (*Lower*) Schematic drawing of an H-segment with C-terminal flanking region.

Results

Model Protein and Topology Assay. As in previous studies (3–6, 18), we have used the *Escherichia coli* inner membrane protein leader

Author contributions: M.L.-B. and G.v.H. designed research; M.L.-B., C.L., H.K., and I.N. performed research; M.L.-B. and G.v.H. analyzed data; and M.L.-B. and G.v.H. wrote the paper.

The authors declare no conflict of interest.

This article is a PNAS Direct Submission.

*To whom correspondence should be addressed. E-mail: gunnar@dbb.su.se.

This article contains supporting information online at www.pnas.org/cgi/content/full/0711580105/DC1.

Table 1. H-segments used in this work

Mutant	Sequence	ΔG_{app} , kcal/mol (batch A)
2L/17A	GGPG**AAAALAAAAAAAAALAAAA**GPGG	0.94
2L/17A-KKKK	GGPG**AAAALAAAAAAAAALAAAA**KKKKGPGG	−0.64
2L/17A-RRRR	GGPG**AAAALAAAAAAAAALAAAA**RRRRGPGG	−0.70
2L/17A-KRKR	GGPG**AAAALAAAAAAAAALAAAA**KRKRGPGG	−0.64
3L/16A	GGPG**AAAALAAAALAAAALAAAA**GPGG	−0.06, 0.33*
3L/16A-K	GGPG**AAAALAAAALAAAALAAAA**KGPGG	0.16
3L/16A-KK	GGPG**AAAALAAAALAAAALAAAA**KKGPGG	−0.16
2L/17A-KK	GGPG**AAAALAAAAAAAAALAAAA**KKGPGG	0.88
2L/17A-KKK	GGPG**AAAALAAAAAAAAALAAAA**KKKGPGG	0.37
2L/19A	GGPG**AAAAAAALAAAAALAAAAAAA**GPGG	0.34
2L/21A	GGPG**AAAAAAAALAAAAALAAAAAAAA**GPGG	−0.19
2L/17A-KKKA	GGPG**AAAALAAAAAAAAALAAAA**KKKAGPGG	0.06
2L/17A-KKKL	GGPG**AAAALAAAAAAAAALAAAA**KKKLGPGG	−0.15
2L/17A-KKKKA	GGPG**AAAALAAAAAAAAALAAAA**KKKKAGPGG	−0.54
2L/17A-KKKKL	GGPG**AAAALAAAAAAAAALAAAA**KKKKLGPGG	−0.61
2L/17A-KAKK	GGPG**AAAALAAAAAAAAALAAAA**KAKKGPGG	0.09
2L/17A-KAKKL	GGPG**AAAALAAAAAAAAALAAAA**KAKKLGPGG	−0.20
2L/17A-KKAK	GGPG**AAAALAAAAAAAAALAAAA**KKAKGPGG	−0.15
2L/17A-KKAKL	GGPG**AAAALAAAAAAAAALAAAA**KKAKLGPGG	−0.22
2L/17A-KAKAK	GGPG**AAAALAAAAAAAAALAAAA**KAKAKGPGG	−0.03
2L/17A-KAKAKL	GGPG**AAAALAAAAAAAAALAAAA**KAKAKLGPGG	−0.34
3L/16A–K(5)	GGPG**(3L/16A)**GPGGKPGQQNATWIVPPGQY	−0.87
3L/16A–K(8)	GGPG**(3L/16A)**GPGGVPGKQNATWIVPPGQY	−0.65
3L/16A–K(13)	GGPG**(3L/16A)**GPGGVPGQQNATKWIVPPGQY	−0.15
3L/16A–K(19)	GGPG**(3L/16A)**GPGGVPGQQNATWIVPPGKY	0.06
3L/16A–K(24)	GGPG**(3L/16A)**GPGGVPGQQNATWIVPPGQYFMMKDNRDNS	0.09
3L/16A–KKK(5)	GGPG**(3L16A)**GPGGKKKPGQQNATWIVPPGQY	−1.72
3L/16A–KKK(8)	GGPG**(3L/16A)**GPGGVPGKKKQNATWIVPPGQY	−1.68
3L/16A–KKK(13)	GGPG**(3L/16A)**GPGGVPGQQNATKKKWIVPPGQY	−1.86
3L/16A–KKK(19)	GGPG**(3L/16A)**GPGGVPGQQNATWIVPPGKKKYFMMGDNRDNS	0.12
3L/16A–KKK(24)	GGPG**(3L/16A)**GPGGVPGQQNATWIVPPGQYFMMKKKDNRDNS	−0.21
3L/16A–KKKKKK(5)	GGPG**(3L/16A)**GPGGKKKKKKPGQQNATWIVPPGQY	−2.60
3L/16A–KKKKKK(8)	GGPG**(3L/16A)**GPGGVPGKKKKKKQNATWIVPPGQY	−2.60
3L/16A–KKKKKK(13)	GGPG(3L16A)GPGGVPGQQNATKKKKKKWIVPPGQY	−2.60
3L/16A–KKKKKK(19)	GGPG**(3L/16A)**GPGGVPGQQNATWIVPPGKKKKKKYFMMGDNRDNS	0.03
3L/16A–KKKKKK(24)	GGPG**(3L/16A)**GPGGVPGQQNATWIVPPGQYFMMKKKKKKDNRDNS	−0.35
$MLT_{(2-26)}$	GGPG**IGAVLKVLTTGLPALISWI**KRKRQQGPGG	−0.09
$MLT_{(2-20)}$	GGPG**IGAVLKVLTTGLPALISWI**GPGG	1.04
L^{15}-$MLT_{(2-26)}$	GGPG**IGAVLKVLTTGLPLLISWI**KRKRQQGPGG	−0.36
L^{15}-$MLT_{(2-20)}$	GGPG**IGAVLKVLTTGLPLLISWI**GPGG	0.63
I^{7}-MLT	GGPG**IGAVLIVLTTGLPALISWI**KRKRQQGPGG	−1.57
$MLT_{(2-21)}$	GGPG**IGAVLKVLTTGLPALISWI**KGPGG	0.86
$MLT_{(2-22)}$	GGPG**IGAVLKVLTTGLPALISWI**KRGPGG	0.69
$MLT_{(2-23)}$	GGPG**IGAVLKVLTTGLPALISWI**KRKGPGG	0.23
$MLT_{(2-24)}$	GGPG**IGAVLKVLTTGLPALISWI**KRKRGPGG	−0.33
L^{15}-$MLT_{(2-21)}$	GGPG**IGAVLKVLTTGLPLLISWI**KGPGG	0.42
L^{15}-$MLT_{(2-22)}$	GGPG**IGAVLKVLTTGLPLLISWI**KRGPGG	0.24
L^{15}-$MLT_{(2-23)}$	GGPG**IGAVLKVLTTGLPLLISWI**KRKGPGG	−0.20
L^{15}-$MLT_{(2-24)}$	GGPG**IGAVLKVLTTGLPLLISWI**KRKRGPGG	−0.42
$MLT_{(2-23)}$L	GGPG**IGAVLKVLTTGLPALISWI**KRKLGPGG	−0.13
$MLT_{(2-24)}$L	GGPG**IGAVLKVLTTGLPALISWI**KRKRLGPGG	−0.01
$MLT_{(2-20)}$-PKRKR	GGPG**IGAVLKVLTTGLPALISWI**PKRKRQQGPGG	0.51
$MLT_{(2-20)}$-KPRKR	GGPG**IGAVLKVLTTGLPALISWI**KPRKRQQGPGG	0.42
$MLT_{(2-20)}$-KRPKR	GGPG**IGAVLKVLTTGLPALISWI**KRPKRQQGPGG	0.32
$MLT_{(2-20)}$-KRKPR	GGPG**IGAVLKVLTTGLPALISWI**KRKPRQQGPGG	0.27
$MLT_{(2-20)}$-KRKRP	GGPG**IGAVLKVLTTGLPALISWI**KRKRRQQGPGG	−0.08

Hydrophobic residues are in bold, inserted charged residues are underlined. Experimentally measured ΔG_{app} values (measured with batch A RMs) or calculated ΔG_{app} values (measured with batch B RMs and then converted as described in *Materials and Methods*) are given; the latter are underlined.

*As seen in a plot of ΔG_{app} values obtained with batch A RMs *vs.* batch B RMs (SI Fig. 6), construct 3L/16A is a little bit off the trend line used for the conversion between the two batches. Therefore, when comparing 3L/16A constructs with other constructs, the relevant value (obtained with batch A or batch B RMs) was always used. The data reported in Fig. 3 were obtained with batch A RMs, and hence the batch A 3L/16A ΔG_{app} value was used to calculate $\Delta\Delta G_{app}$ values, whereas in all other cases the batch B 3L/16A ΔG_{app} value was used to calculate $\Delta\Delta G_{app}$ values.

peptidase (Lep) as the model protein. Lep consists of two transmembrane segments (TM1, TM2) connected by a short cytoplasmic loop (P1) and a large C-terminal domain (P2). The protein inserts into ER-derived dog pancreas rough microsomes (RMs) with both termini located in the lumen (19) (Fig. 1). Potential transmembrane segments (H-segments) are introduced in the P2 domain in a location where they are flanked on both sides by Asn-X-Thr acceptor sites for N-linked glycosylation

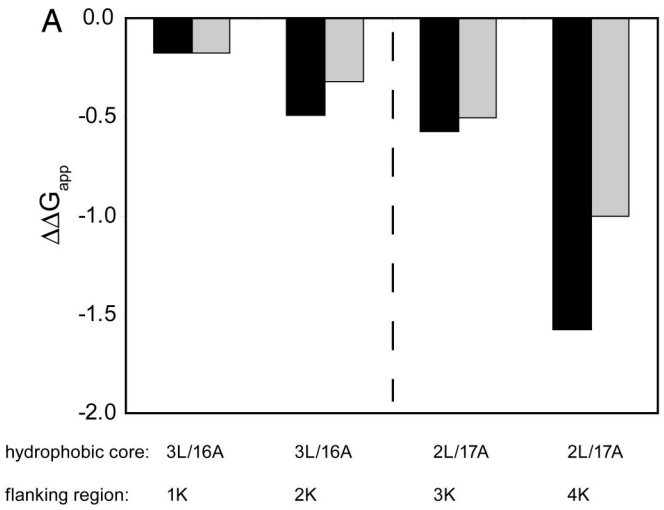

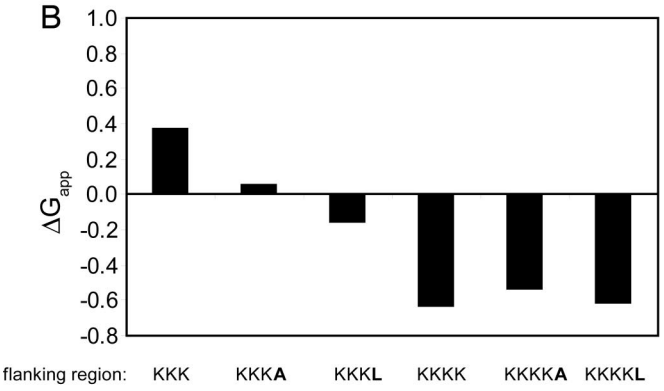

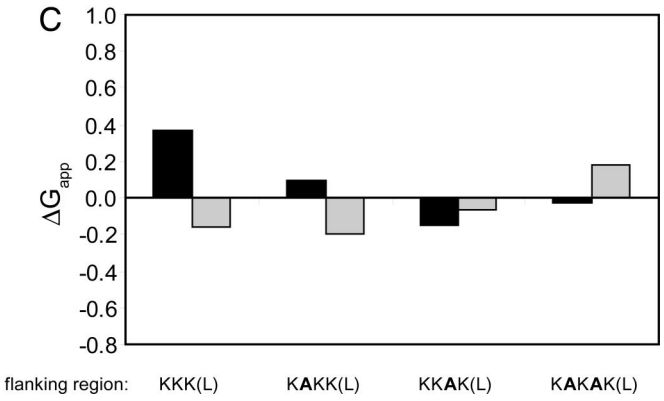

Fig. 2. Membrane insertion of Ala/Leu-based H-segments with C-terminal positively charged flanking residues. (*A*) $\Delta\Delta G_{app}$ relative to the indicated core H-segment for 1–4 Lys residues (black bars) and $\Delta\Delta G_{app}$ for the last added Lys residue (gray bars). Data obtained with 3L/16A and 2L/17A H-segments are separated by a dashed line. (*B*) ΔG_{app} for 2L/17A/*n*K H-segments ($n = 3, 4$) with and without a C-terminal Ala or Leu residue. (*C*) ΔG_{app} for 2L/17A/(3K, *n*A) H-segments (black bars). Same constructs but with an added C-terminal Leu residue (gray bars).

(G1, G2). After *in vitro* transcription–translation in the presence of RMs, the degree of membrane insertion of the H-segment is quantified by comparing the fractions of singly glycosylated (i.e., membrane-integrated) and doubly glycosylated (i.e., nonintegrated) molecules, which we express as an apparent free energy of membrane insertion, ΔG_{app} (see *Materials and Methods*). Given the complexity of the *in vitro* system, the noninserted state cannot be precisely defined but presumably corresponds to an

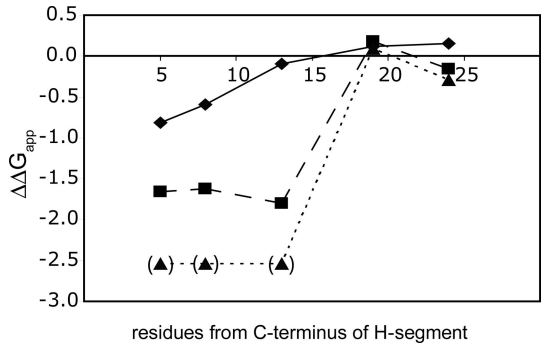

Fig. 3. Distance dependence of the effect of charged flanking residues. ΔG_{app} values for a 3L/16A H-segment with one (diamonds), three (squares) or six (triangles) consecutive Lys residues placed at increasing distances from the hydrophobic segment. The 6K constructs indicated in parentheses are essentially fully membrane-inserted, and their ΔG_{app} values cannot be determined accurately.

H-segment exposed to the aqueous environment within or just outside the translocon channel (1, 2).

In this work, the H-segments are all composed of a 19- to 23-residue-long hydrophobic stretch and a C-terminal 0- to 6-residue-long flanking segment containing positively charged residues. To "insulate" the H-segment (including the charged flanking residues) from the surrounding sequence, it is delimited by N- and C-terminal GGPG... GPGG stretches. All H-segments analyzed are listed in Table 1.

C-Terminal Positively Charged Residues Promote Insertion of Ala/Leu-Based H-Segments. We first compared the effects of Lys and Arg on H-segment insertion by using a 2L/17A hydrophobic core segment immediately followed by one of three different positively charged segments: KKKK, RRRR, or KRKR. All three charged segments were found to favor insertion to the same extent ($\Delta\Delta G_{app} = -1.6$ kcal/mol compared with the 2L/17A segment lacking charged flanking residues; Table 1). Because Lys and Arg residues have virtually identical effects, only Lys residues were used in all subsequent experiments.

H-segments of the composition 3L/16A and 2L/17A with 1–4 C-terminal Lys residues were analyzed next. ΔG_{app} decreased monotonically as more charged residues were added (Fig. 2*A*) (note that the composition of the H-segment was chosen such that ΔG_{app} is within the interval $[-1, +1]$ kcal/mol whenever possible because the measurement error is smallest in this interval). Because it was shown that ΔG_{app} decreases proportionally to the length of the H-segment (6) and given that the long lysine side chain can "snorkel" along the transmembrane helix (20–22), the question arises whether the observed effect is partly caused by the increase in length of the hydrophobic part of the H-segment provided by the nonpolar part of the lysine side chains. To address this possibility, we analyzed constructs with longer hydrophobic stretches but no flanking charges. Elongation of the 2L/17A H-segment by 2 alanines gives the same reduction in ΔG_{app} as does the addition of 2 lysines to the 3L/16A H-segment ($\Delta\Delta G_{app} = -0.6$ and -0.5 kcal/mol, respectively) (Table 1). The addition of 2 more alanines (construct 2L/21A) increases the insertion efficiency in a linear manner ($\Delta\Delta G_{app}$ -1.1 kcal/mol relative to 2L/17A), whereas the addition of 2 more lysines leads to a larger reduction in $\Delta\Delta G_{app}$(-1.6 kcal/mol relative to 2L/17A). As seen in Fig. 2*A*, each of the first 3 lysines lowers the free energy of insertion by -0.2 to -0.5 kcal/mol per added residue, whereas the value is considerably larger for the 4th lysine ($\Delta\Delta G_{app} = -1.0$ kcal/mol). Although the chemically rather complex lysine side chain can engage in both nonpolar and polar interactions, the positive charge *per se* clearly causes an

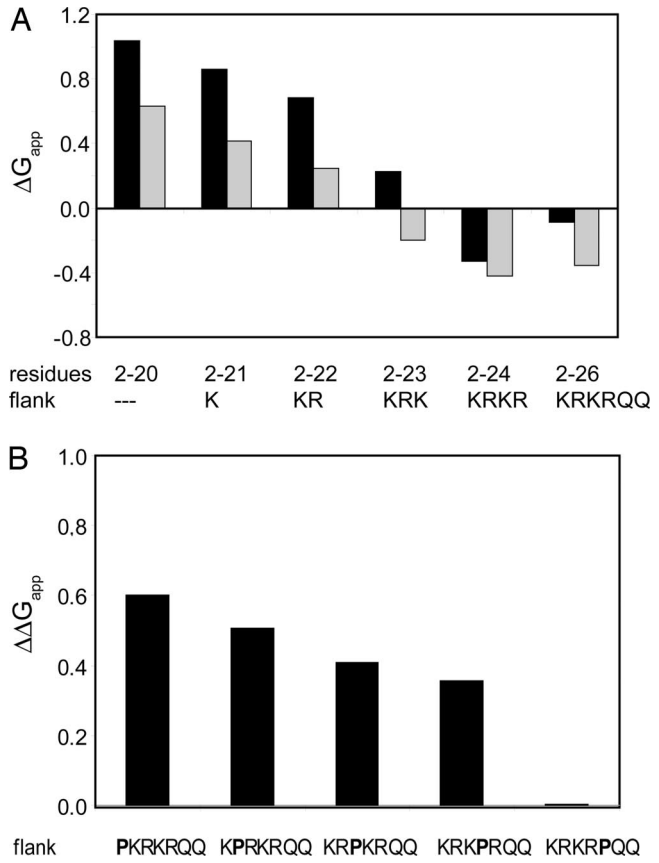

Fig. 4. Membrane insertion of melittin-derived H-segments. (*A*) ΔG_{app} values for melittin segments including different lengths of the natural flanking segment (black bars) and for segments with an additional A15L mutation (gray bars). (*B*) $\Delta\Delta G_{app}$ values relative to MLT_{2-26} for Pro insertions in the flanking segment.

increase in the insertion efficiency, at least when it is placed a few residues away from the H-segment.

To minimize the possible influence from side-chain snorkeling, we further placed 1 or 3 lysines immediately downstream of the "insulating" GPGG residues. Again, the effect on ΔG_{app} was strong: a single lysine reduced ΔG_{app} for the 3L/16A H-segment by -0.8 kcal/mol and 3 lysines reduced ΔG_{app} by -1.7 kcal/mol (Table 1).

To examine the difference in $\Delta\Delta G_{app}$ between 3 and 4 added lysines more closely, we made constructs with an additional hydrophobic residue (Leu or Ala) just after the charge cluster (but before the GPGG stretch). Presumably, with only a few lysines between the hydrophobic segment and the additional hydrophobic residue, the latter can enhance membrane insertion through interaction of the hydrophobic side chain with the membrane (21, 22). Indeed, insertion of an Ala or Leu residue after a block of 3 consecutive lysines reduces ΔG_{app} by -0.3 and -0.5 kcal/mol, respectively (Fig. 2*B*). When introduced after a block of 4 lysines, however, the Ala or Leu residue does not increase the insertion efficiency.

The introduction of an Ala residue in positions between the 3 lysines has a similar effect and reduces ΔG_{app} by approximately -0.3 kcal/mol (Fig. 2*C*), and the further addition of a downstream Leu residue again reduces ΔG_{app} by an extra -0.3 kcal/mol (except for the KKAK flank, where the insertion of the Ala residue in itself has an unexpectedly large effect).

Distance Dependence of the Effect of Positively Charged Residues on ΔG_{app}. Because the results presented above indicate that a positively charged residue has a maximal effect on ΔG_{app} when placed at a certain distance away from the H-segment, we performed a "lysine scan" in which 1, 3, or 6 consecutive lysines were placed at different positions downstream of the GPGG stretch in a 3L/16A H-segment.

As seen in Fig. 3, a single lysine still has an appreciable effect on ΔG_{app} when placed 8 residues downstream of the GPGG stretch but not when placed 13 residues away. For the 3K and 6K stretches, a strong effect is seen also for a distance of 13 but not 19 residues.

Effects of Positively Charged Residues on the Membrane Insertion of a Melittin-Derived Transmembrane Segment. To complement our studies of the effect of charged flanking residues on the insertion of simple model H-segments, we also investigated the importance for membrane insertion of the natural KRKR charge cluster at the C terminus of melittin, a well characterized membrane-active peptide from bee venom. Again, we introduced various melittin-derived H-segments into Lep. As seen in Table 1, an H-segment representing full-length melittin (MLT_{2-26}) inserted with a ΔG_{app} of -0.1 kcal/mol ($\approx$50% of the molecules inserted), whereas truncated melittin (MLT_{2-20}) without the C-terminal KRKRQQ flank hardly inserted at all ($\Delta G_{app} = 1.0$ kcal/mol). The positively charged residues are therefore essential for insertion of the melittin-derived H-segment. Because the value for MLT_{2-20} is at the border of the sensitive range of the assay and thus associated with a higher uncertainty in the ΔG_{app} value, we introduced an A15L mutation (L^{15}-MLT_{2-26} and L^{15}-MLT_{2-20}) and confirmed that the favorable effect of the positively charged flanking region is approximately -1.1 kcal/mol also in this case (Table 1). The $\Delta\Delta G_{app}$ caused by the A15L mutation itself was -0.3 for the MLT_{2-26} and -0.4 for MLT_{1-20}, in good agreement with the $\Delta\Delta G_{app}$ of -0.55 kcal/mol predicted by the biological hydrophobicity scale (3).

In biophysical model systems, the strongly amphiphilic melittin peptide binds to the membrane surface before insertion and channel formation. In our assay, binding of an amphiphilic H-segment to the membrane surface could possibly inhibit glycosylation by making the G2 glycosylation site, which is close to the H-segment, partly inaccessible to the oligosaccharyl transferase. To address this possibility, we performed a proteinase K protection assay on I^{7}-MLT_{2-26}, a very efficiently inserting melittin mutant, and on MLT_{2-20}. As seen in supporting information (SI) Fig. 5, the unglycosylated P2 domain of I^{7}-MLT_{2-26} is digested by proteinase K and hence located outside the microsomes, as expected. In contrast, the glycosylated P2 domain of MLT_{2-20} is protected and hence located in the lumen, again as expected from its glycosylation status. The results are very similar to those obtained for a series of Ala/Leu H-segments with varying insertion efficiencies. We conclude that quantifications based on glycosylation efficiencies are reliable even for amphiphilic H-segments such as those derived from melittin.

We next investigated how the insertion efficiency of the melittin-derived H-segments relates to the number of charged residues in the C-terminal flank (Fig. 4*A*). For both MLT and L^{15}-MLT, there is an approximately linear increase in insertion efficiency with the number of charged residues, with a reduction in ΔG_{app} -0.1 to -0.3 kcal/mol per residue, similar to the increase observed for the simple Ala/Leu-based model sequences above. By contrast, the 2 Gln after the 4 charged residues have little or no effect on insertion.

We also checked for a modulation of this effect when the charge cluster is followed by an additional Leu. As found for the simple Ala/Leu-based constructs, a Leu after 3 charged residues favors insertion ($\Delta\Delta G_{app} = -0.4$ kcal/mol), whereas when the Leu residue is placed after 4 charged residues there is no such favorable effect (Table 1).

Finally, to investigate whether the favorable effect of flanking positively charged residues requires that the charge cluster is in a

helical conformation, we introduced a helix-breaking proline at different positions in the flanking region (Fig. 4*B*). Strikingly, by placing a Pro between the hydrophobic stretch and the charged flanking region, 0.6 kcal/mol of insertion free energy is lost. The energetic cost is gradually decreased by shifting the proline further into the charged flank. To promote membrane insertion efficiently, a helical structure of the charged flanking region seems optimal.

Discussion

Although hydrophobicity is the overriding characteristic that determines whether or not a polypeptide segment is recognized as a transmembrane α-helix during passage through the Sec61 translocon in the ER, the membrane insertion efficiency can be modulated by residues flanking the hydrophobic stretch. In particular, charged flanking residues have been shown to either reduce or enhance membrane insertion, with luminal negatively charged or strongly polar flanking residues reducing insertion and cytosolic positively charged residues enhancing insertion (6, 23).

Here, we report a quantitative study of the effects on membrane insertion of positively charged residues placed near the cytoplasmic end of model transmembrane segments (H-segments). Overall, our results show (*i*) that flanking Lys and Arg residues contribute equally to the apparent free energy of membrane insertion (ΔG_{app}), (*ii*) that the effect is maximal when the charged residues are placed a few residues away from the H-segment, (iii) that a hydrophobic residue added immediately downstream of a contiguous stretch of *n* Lys residues contributes favorably to ΔG_{app} only if $n \leq 3$, (*iv*) that a helix-breaking Pro residue reduces the contribution to ΔG_{app} from downstream positively charged residues, and (*v*) that a stretch of 3 or 6 consecutive Lys residues can contribute significantly to ΔG_{app} from a distance of up to $\approx$13 residues away from the hydrophobic segment. There is a striking similarity between these result and the effect exerted by positively charged residues on the orientation of transmembrane α-helices, where stretches of Lys or Arg residues have been shown to promote a cytosolic location when located up to $\approx$25 residues away from the hydrophobic transmembrane segment (23, 24).

The results are consistent with the positive inside rule, which states that positively charged residues tend to be enriched near the cytosolic end of transmembrane helices (12). As shown here, positively charged residues significantly enhance the membrane insertion capability of a weakly hydrophobic segment, typically contributing approximately -0.5 kcal/mol per residue to ΔG_{app}, but only when placed at the cytosolic end of the segment (6). Because Asp, Glu, Asn, Gln, or Ser residues placed at the cytosolic end of an H-segment have no effect on ΔG_{app} compared with Gly residues (6), the positive charge on the Lys or Arg side chain must provide the major part of the stabilization.

Given the amphiphilic nature of the Lys and Arg side chains and the complexity of the Sec61 translocon, the detailed molecular mechanism behind these phenomena remains unclear. Some guidance may be provided by our previous finding that the contribution to ΔG_{app} is to a good approximation independent of position within the H-segment for hydrophobic residues but depends strongly on position for charged residues (6). Therefore, the contribution from the positively charged moiety in the Lys side chain is expected to change from destabilizing to stabilizing over a narrow region near the end of the H-segment, whereas the contribution from the side-chain methylenes should be rather constant, consistent with our observation that the addition of Ala residues at the end of the H-segment results in a linear decrease in ΔG_{app}, whereas the contribution from a Lys residue increases with the number of lysines already added (Fig. 2*A*).

We also find that the Lys residues placed immediately downstream of the H-segment contribute the most to ΔG_{app} when they form a continuation of the transmembrane helix, as demonstrated by the increase in ΔG_{app} seen when a helix-breaking Pro residue is introduced into the charged C-terminal stretch in melittin (Fig. 4*B*). A helical conformation may also explain the observation that the addition of a hydrophobic residue immediately downstream of a Lys-stretch reduces ΔG_{app} when preceded by up to 3 but not by 4 lysines (Fig. 2*B*). In the latter case, there is a full helix turn of Lys residues (a "picket fence") preventing back-snorkeling of the hydrophobic residue along the helix. A helical conformation ensures a high density of positively charged residues near the cytoplasmic end of the transmembrane helix and may facilitate favorable electrostatic interactions with either negatively charged lipid headgroups or negatively charged residues in the Sec61 translocon itself (25, 26). However, Lys residues can promote membrane insertion also when they are more distant from the hydrophobic stretch and presumably do not form an extension of the transmembrane helix (Fig. 3). Similar long-range effects exerted by Lys residues on the orientation (rather than membrane insertion) of an N-terminal transmembrane helix have been suggested to involve a direct interaction between the charged residues and the Sec61 translocon (23).

Beyond the conceptual issues concerning the mechanism of membrane insertion, we note that the availability of quantitative experimental data on the contribution of positively charged residues to ΔG_{app} will make it possible to refine membrane protein topology-prediction methods further based on free-energy calculations.

Materials and Methods

Enzymes and Chemicals. All enzymes, plasmid pGEM1, and the TNT Quick transcription–translation system were from, Invitrogen or Promega. [^{35}S]Methionine and deoxynucleotides were from GE Healthcare. The Big Dye Terminator version 1.1 cycle sequencing kit was from Applied Biosystems. Oligonucleotides were obtained from Cybergene and MWG Biotech.

Expression *in Vitro* and Quantification of Membrane Insertion Efficiency. All plasmids were constructed as described in ref. 3, and insertion of single amino acids was performed with site-directed mutagenesis (Stratagene). The sequence of all constructs was confirmed by sequencing of plasmid DNA at BM labbet. Constructs cloned in pGEM1 were transcribed and translated in the TNT Quick coupled transcription–translation system. One microgram of DNA template, 1 μl of [^{35}S]Met (5 μCi) and 1 μl of EDTA stripped, nuclease-treated dog pancreas rough microsomes [gifts from M. Sakaguchi, Hyogo University (batch A) and B. Dobberstein, ZMBH Heidelberg (batch B)] were added at the start of the reaction, and samples were incubated for 90 min at 30°C. Translation products were analyzed by SDS/PAGE, and gels were quantified on a Fuji FLA-3000 PhosphorImager with Image Reader 8.1j software. The degree of membrane integration of each H-segment was quantified from SDS/polyacrylamide gels by calculating an apparent equilibrium constant between the membrane-integrated and nonintegrated forms: $K_{app} = f_{1g}/f_{2g}$, where f_{1g} is the fraction of singly and f_{2g} the fraction of doubly glycosylated Lep molecules after correcting for the fact that a fully translocated P2 domain is only glycosylated to $\approx$85% for the batch A microsomes (3); no such correction was used for batch B. The results were then converted to apparent free energies, $\Delta G_{app} = -RT \ln K_{app}$. All reported ΔG_{app} values are mean values from at least two independent experiments; for H-segments with $\Delta G_{app} \in [-1, +1]$ kcal/mol, the expected precision in the ΔG_{app} values is approximately $\pm$ 0.2 kcal/mol (3). Seventeen constructs were analyzed with both batches of microsomes. The least-squares linear correlation between the two sets of ΔG_{app} values is good ($R^2 = 0.89$) and given by $\Delta G_{app}^{\text{batch A}} = 0.77\ \Delta G_{app}^{\text{batch B}} - 0.13$ kcal/mol (SI Fig. 6). Table 1 presents measured or calculated (by using the above equation for constructs analyzed with batch B microsomes) ΔG_{app} values for batch A microsomes. Batch A microsomes were used in our previous studies, e.g., refs. 3 and 6.

ACKNOWLEDGMENTS. This work was supported by a grant from the Swiss National Science Foundation (to M.L.-B.); by grants from the Carl Trygger Stiftelse and Magnus Bergvalls Stiftelse (to I.N.); and by grants from the Swedish Research Council, the Marianne and Marcus Wallenberg Foundation, the Swedish Foundation for Strategic Research, and the Swedish Cancer Foundation (to G.v.H.).

1. Alder NN, Johnson AE (2004) Cotranslational membrane protein biogenesis at the endoplasmic reticulum. *J Biol Chem* 279:22787–22790.
2. Rapoport TA (2007) Protein translocation across the eukaryotic endoplasmic reticulum and bacterial plasma membranes. *Nature* 450:663–669.
3. Hessa T, *et al*. (2005) Recognition of transmembrane helices by the endoplasmic reticulum translocon. *Nature* 433:377–381.
4. Hessa T, White SH, von Heijne G (2005) Membrane insertion of a potassium channel voltage sensor. *Science* 307:1427.
5. Meindl-Beinker NM, Lundin C, Nilsson I, White SH, von Heijne G (2006) Asn- and Asp-mediated interactions between transmembrane helices during translocon-mediated membrane protein assembly. *EMBO Rep* 7:1111–1116.
6. Hessa T, *et al*. (2007) Molecular code for transmembrane-helix recognition by the Sec61 translocon. *Nature* 450:1026–1030.
7. Wimley WC, Creamer TP, White SH (1996) Solvation energies of amino acid side chains and backbone in a family of host–guest pentapeptides. *Biochemistry* 35:5109–5124.
8. Ulmschneider MB, Sansom MS, Di Nola (2005) Properties of integral membrane protein structures: Derivation of an implicit membrane potential. *Proteins* 59:252–265.
9. van den Berg B, *et al*. (2004) X-ray structure of a protein-conducting channel. *Nature* 427:36–44.
10. Li W, *et al*. (2007) The plug domain of the SecY protein stabilizes the closed state of the translocation channel and maintains a membrane seal. *Mol Cell* 26:511–521.
11. Higy M, Junne T, Spiess M (2004) Topogenesis of membrane proteins at the endoplasmic reticulum. *Biochemistry* 43:12716–12722.
12. von Heijne G (1986) The distribution of positively charged residues in bacterial inner membrane proteins correlates with the trans-membrane topology. *EMBO J* 5:3021–3027.
13. von Heijne G (1989) Control of topology and mode of assembly of a polytopic membrane protein by positively charged residues. *Nature* 341:456–458.
14. von Heijne G (1986) Net N–C charge imbalance may be important for signal sequence function in bacteria. *J Mol Biol* 192:287–290.
15. Habermann E, Jentsch J (1967) Sequence analysis of melittin from tryptic and peptic degradation products. *Hoppe Seylers Z Physiol Chem* 348:37–50.
16. Sitaram N, Nagaraj R (1999) Interaction of antimicrobial peptides with biological and model membranes: Structural and charge requirements for activity. *Biochim Biophys Acta* 1462:29–54.
17. Bechinger B, Lohner K (2006) Detergent-like actions of linear amphipathic cationic antimicrobial peptides. *Biochim Biophys Acta* 1758:1529–1539.
18. Sääf A, Wallin E, von Heijne G (1998) Stop-transfer function of pseudo-random amino acid segments during translocation across prokaryotic and eukaryotic membranes. *Eur J Biochem* 251:821–829.
19. Johansson M, Nilsson I, von Heijne G (1993) Positively charged amino acids placed next to a signal sequence block protein translocation more efficiently in *Escherichia coli* than in mammalian microsomes. *Mol Gen Genet* 239:251–256.
20. Monné M, von Heijne G (2001) Effects of ''hydrophobic mismatch'' on the location of transmembrane helices in the ER membrane. *FEBS Lett* 496:96–100.
21. Chamberlain AK, Lee Y, Kim S, Bowie JU (2004) Snorkeling preferences foster an amino acid composition bias in transmembrane helices. *J Mol Biol* 339:471–479.
22. Granseth E, von Heijne G, Elofsson A (2005) A study of the membrane–water interface region of membrane proteins. *J Mol Biol* 346:377–385.
23. Kida Y, Morimoto F, Mihara K, Sakaguchi M (2006) Function of positive charges following signal-anchor sequences during translocation of the N-terminal domain. *J Biol Chem* 281:1152–1158.
24. Hermansson M, Monné M, von Heijne G (2001) Formation of helical hairpins during membrane protein integration into the endoplasmic reticulum membrane: Role of the N, C-terminal flanking regions. *J Mol Biol* 313:1171–1179.
25. Goder V, Junne T, Spiess M (2004) Sec61p contributes to signal sequence orientation according to the positive-inside rule. *Mol Biol Cell* 15:1470–1478.
26. Junne T, Schwede T, Goder V, Spiess M (2007) Mutations in the Sec61p channel affecting signal sequence recognition and membrane protein topology. *J Biol Chem* 282:33201–33209.